Topological entanglement entropy of interacting disordered zigzag graphene ribbons

Young Heon Kim [ORCID],[*] Hye Jeong Lee [ORCID],[*] and S.-R. Eric Yang [ORCID][†]

Department of Physics, Korea University, Seoul 02855, Korea

Interacting disordered zigzag graphene nanoribbons have fractional charges, are quasi-one-dimensional, and display an exponentially small gap. Our numerical computations showed that the topological entanglement entropy of these systems has a small finite but universal value, independent of the strength of the interaction and the disorder. The result that was obtained for the topological entanglement entropy shows that the disorder-free phase is critical and becomes unstable in the presence of disorder. Our result for the entanglement spectrum in the presence of disorder is also consistent with the presence of a topologically ordered phase.

I. INTRODUCTION

Graphene structures have many fascinating physical properties, such as massless Dirac electrons and the quantum Hall effect [1–4]. Recent years have seen rapid progress in the fabrication of atomically precise graphene nanoribbons [5]. Recent studies showed [6,7] that interacting zigzag graphene nanoribbons [8] are topologically ordered [9,10] when disorder is present. The ground states of these quasi-one-dimensional Mott-Anderson insulators are doubly degenerate: the two degenerate ground states are related to each other in that their electron spins are reversed (see Fig. 1). They have an exponentially small gap, Δ_s, in the density of states (DOS) (see Fig. 2) and their boundary zigzag edges can support $1/2$ fractional charges. These objects are solitonic in nature [11,12]. Moreover, the zigzag edges induce spin splitting in the bulk [13] and can display spin-charge separation. Disorder in interacting zigzag graphene ribbons induces a transition between symmetry-protected and topologically ordered phases.

In this paper, we investigated the entanglement in many-body topological insulators [14,15] of interacting disordered zigzag graphene nanoribbons. A region D of a topologically ordered *gapful* system with *one* boundary has an entanglement entropy [16–18]

$$S_D = \alpha L - \beta \tag{1}$$

with the subdominant and universal topological entanglement entropy (TEE) $\beta > 0$ [19,20]. The value of β can be numerically computed, see, for example, Jiang *et al.* [21]. Here L is the length of the boundary and α is nonuniversal constant. The entanglement entropy $S_D = -\text{Tr}[\rho_D \ln \rho_D]$ is given by the reduced density matrix ρ_D of region D.

In the case of non-negligible finite-size effects and disorder fluctuations, different methods can be used to compute β. We adopt the method of partitioning the system into different

regions [19,20]. The TEE of a ring [20] can be written as

$$S_{\text{top}} = 2\beta = -[(S_A - S_B) - (S_C - S_D)]. \tag{2}$$

S_A is the entanglement entropy for the region consisting of the sites in A. Other entanglement entropies defined similarly. The regions should be as in Fig. 3 or a smooth deformation thereof without changing how the regions border on each other. The entanglement entropy $S_A - S_B$ has the contribution as that of $S_C - S_D$. The difference between these two contributions is the TEE. Note that other regions have only one boundary, whereas A has *two* boundaries, i.e., one inner and one outer, as shown in Fig. 3. Except near a *critical point*, the value of the TEE is universal and is independent of system parameters.

Several questions regarding the entropy of interacting disordered zigzag ribbons remain unanswered. For example, it is unclear whether these ribbons should have nonzero TEE. As mentioned above, the presence of fractional charges suggests that the TEE is finite, although the magnitude thereof is unknown. However, the presence of an exponentially small gap may be compatible with zero TEE. In addition, the behavior of the TEE near the critical point is unclear. In this paper, we numerically computed the TEE and showed that it is finite and universal, and independent of the strength of both the interaction and disorder. Our results also showed that the disorder-free phase is critical and that this phase becomes unstable in the presence of disorder.

II. MODEL

We applied a Hubbard model to the interacting disordered zigzag graphene nanoribbons and used a self-consistent Hartree-Fock approximation [15,22]. We included both electron–electron interactions and disorder in a tight-binding model at half-filling. When the on-site repulsion is $U = 0$, the effect of disorder can be described exactly within the Hartree-Fock approximation whereas, in the other limit, where disorder is absent, the interaction effects are well represented by the Hartree-Fock approximation, which is widely used in graphene-related systems [23]. The ground

---

[*]These authors contributed equally to this work.

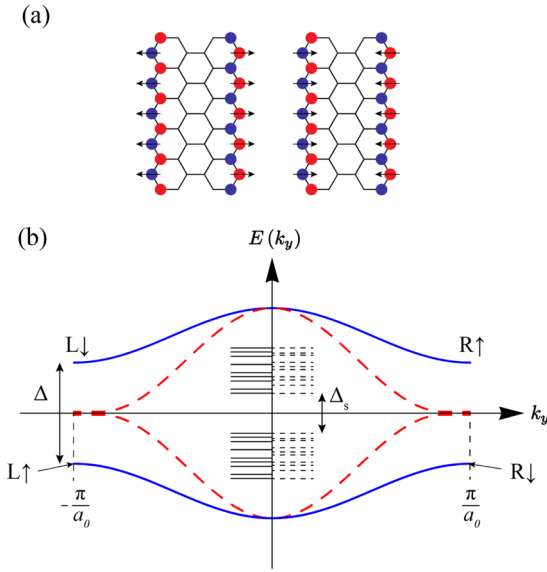[†]Corresponding author: eyang812@gmail.com

(a)

(b)

FIG. 1. (a) Zigzag edge antiferromagnetism of an interacting zigzag graphene nanoribbon without disorder showing the two degenerate ground states. (b) Schematic band structures of interacting (solid curves) and noninteracting (dashed curves) zigzag graphene nanoribbons. Unoccupied and occupied states near the wave vectors $k = \pm\pi/a_0$: R and L represent the states confined to the zigzag edges on the right and left, respectively (the length of the unit cell of a ribbon is a_0). The small arrows indicate the spins. Spin-split energy levels of the spin-up (solid lines) and spin-down (dashed lines) *gap-edge* states of the interacting disordered interacting zigzag graphene nanoribbons. These figures are taken from Ref. [7].

state is doubly degenerate and can be written as a product of spin-up and -down Slater determinants,

$$\Psi_1 = \Psi_{L,\uparrow}(\vec{r}_1, \ldots, \vec{r}_{N/2})\Psi_{R,\downarrow}(\vec{r}_{N/2+1}, \ldots, \vec{r}_N),$$

$$\Psi_2 = \Psi_{R,\uparrow}(\vec{r}_1, \ldots, \vec{r}_{N/2})\Psi_{L,\downarrow}(\vec{r}_{N/2+1}, \ldots, \vec{r}_N), \quad (3)$$

where $\Psi_{L,\sigma}$ ($\Psi_{R,\sigma}$) describes $N/2$ electrons with spin σ with some of these electrons localized on the left (right) zigzag edge. In the first state, the spin of the magnetization of the zigzag edge on the left (right) is dominantly upward (downward), see Fig. 1(a). In the second state, the magnetization is the opposite. The total number of electrons is N. In these wave functions, spins are separated because spin terms of the mean-field Hamiltonian are separated, $H = H_\uparrow + H_\downarrow$ [6,7], see the following equation.

The total Hamiltonian in the Hartree-Fock approximation is

$$H = -\sum_{\langle ij \rangle \sigma} t c_{i\sigma}^\dagger c_{j\sigma} + \sum_{i\sigma} V_i c_{i\sigma}^\dagger c_{i\sigma}$$

$$+ U \sum_i (n_{i\uparrow}\langle n_{i\downarrow}\rangle + \langle n_{i\uparrow}\rangle n_{i\downarrow} - \langle n_{i\uparrow}\rangle\langle n_{i\downarrow}\rangle)$$

$$- \frac{U}{2}\sum_i (n_{i\uparrow} + n_{i\downarrow}), \quad (4)$$

where $c_{i\sigma}^\dagger$ and $n_{i\sigma}$ are the electron creation and occupation operators at site i with spin σ. Because the translational

symmetry is broken, the Hamiltonian is written in the site representation. In the hopping term, the summation is over the nearest-neighbor sites (the value of the hopping parameter is $t \sim 3$ eV). The eigenstates and eigenenergies are computed numerically by solving the tight-binding Hamiltonian matrix self-consistently. The self-consistent occupation numbers $\langle n_{i\sigma}\rangle$ in the Hamiltonian are the sum of the probabilities of finding electrons of spin σ at site i:

$$\langle n_{i\sigma}\rangle = \sum_{E \leqslant E_F} |\psi_{i\sigma}(E)|^2. \quad (5)$$

The summation is over the energy E of the occupied eigenstates below the Fermi energy E_F. Note that $\psi_{i\sigma}(E)$ represents an eigenvector of the tight-binding Hamiltonian matrix with energy E. The on-site impurity energy V_i is chosen randomly from the energy interval $[-\Gamma, \Gamma]$.

III. CALCULATION OF TOPOLOGICAL ENTANGLEMENT ENTROPY

The upward or downward spin destruction operator of a Hartree-Fock single-particle state $|k\rangle$ is

$$a_k = \sum_i \mathbf{A}_{ki} c_i, \quad (6)$$

where c_i is the destruction of the operator at site i. Inverting this relation, we find

$$c_i = \sum_k (\mathbf{A}^{-1})_{ik} a_k = \sum_k \mathbf{B}_{ik} a_k. \quad (7)$$

Let us divide the zigzag ribbon into two parts A and B. We restrict the indices i and j to A and define the correlation function/reduced density matrix [24,25],

$$\mathbf{C}_{ij} = \langle \Psi | c_i^+ c_j | \Psi \rangle, \quad (8)$$

where $\Psi = \Psi_1$ is chosen (Ψ_2 is an equally good choice). This can be written as

$$\mathbf{C}_{ij} = \langle \Psi | \left(\sum_k \mathbf{B}_{ik} a_k\right)^+ \left(\sum_{k'} \mathbf{B}_{jk'} a_{k'}\right) | \Psi \rangle$$

$$= \langle \Psi | \left(\sum_k a_k^+ \mathbf{B}_{ki}^*\right) \left(\sum_{k'} \mathbf{B}_{jk'} a_{k'}\right) | \Psi \rangle$$

$$= \sum_k \mathbf{B}_{ki}^* \mathbf{B}_{jk} n_k. \quad (9)$$

Here we have used

$$\langle \Psi | a_k^+ a_{k'} | \Psi \rangle = \delta_{kk'} n_k, \quad (10)$$

where n_k is the number of occupied Hartree-Fock states. The entanglement entropy of A is given by

$$S_A = -\sum_i [\lambda_i \ln\lambda_i + (1-\lambda_i)\ln(1-\lambda_i)], \quad (11)$$

where λ_i are the eigenvalues of the matrix $\mathbf{C}$.

IV. TOPOLOGICAL ENTANGLEMENT ENTROPY

We computed S/L as a function of $1/L$ and tried to extract the TEE from the result. For an interacting but disorder-
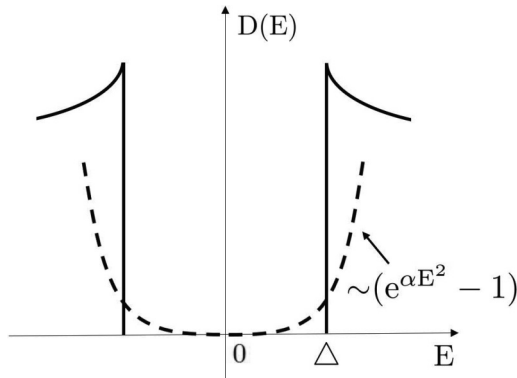
FIG. 2. Dashed line: The exponentially small *soft* gap with $\alpha \sim 1/\sqrt{\Delta_s}$ near the Fermi energy of the tunneling density of states of an interacting disordered zigzag graphene nanoribbon. Solid line: The *hard* gap, Δ, of the tunneling density of states of an interacting zigzag graphene nanoribbon in the absence of disorder.

free system, we found $\beta \approx 0$. Note that, in this case, a hard gap exists in the DOS and *no* zero-energy zigzag edge states exist, as shown in Fig. 2. However, in the presence of disorder, the method for computing the TEE from Eq. (1) is not accurate: the data we obtained display significant disorder fluctuations that depend on the size of the system.

We use another method based on a rectangular ring to compute $S_{\text{top}} = 2\beta$ given in Eq. (2). Since the whole ribbon is topologically ordered [6,7], we can divide the system into a rectangular ring that lies well inside the ribbon and the rest of the ribbon. However, a careful analysis is required to reduce finite-size effects, see Jiang *et al.* [21]. For this purpose, we adopt the partition of the ribbon shown in Fig. 3 [20]. We apply this method to compute β of interacting disordered zigzag ribbons. To compute β, one must use a thick and large rectangular ring. The width of the ring
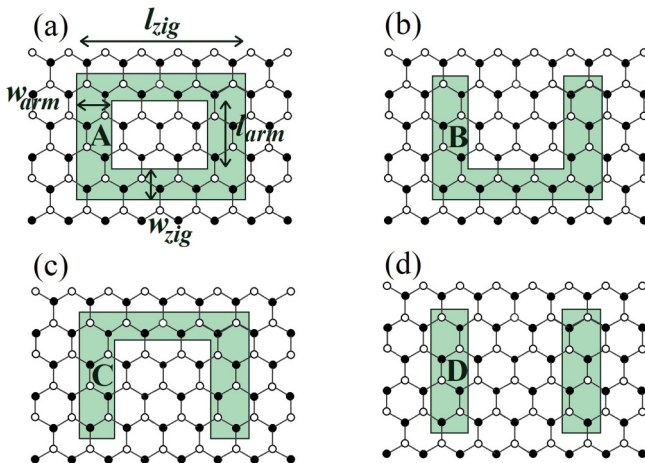

FIG. 3. Different regions of the ribbon used in Eq. (2) to compute the TEE. Vertical lengths are measured in number of horizontal carbon lines and horizontal lengths in number of vertical carbon lines.
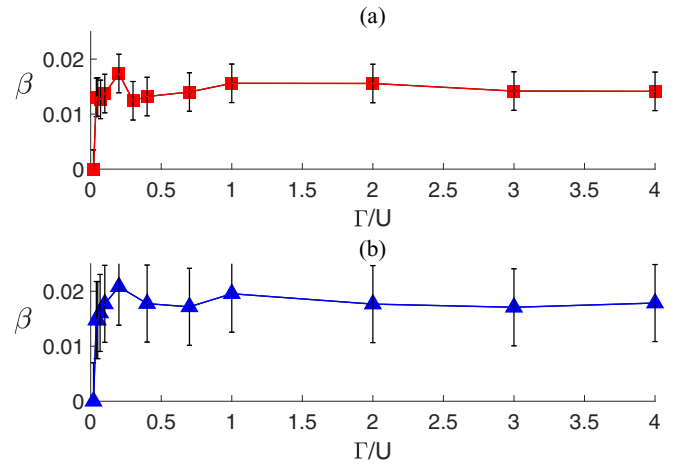

FIG. 4. TEE β of an interacting disordered zigzag nanoribbon is computed using a rectangular ring with different ring widths w. Each point represents a different value of (U, Γ). In (a), the ring width, ribbon length, ribbon width are, respectively, $w = 7$, $L' = 260$, $W = 112$. The side lengths of the ring are $l_{\text{zig}} = 221$ and $l_{\text{arm}} = 46$. In (b), they are $w = 4$, $L' = 200$ $W = 64$, $l_{\text{zig}} = 161$, $l_{\text{arm}} = 28$. The number of disorder realizations N_D are, respectively, 10 and 20 in (a) and (b).

$w = w_{\text{zig}} = w_{\text{arm}}$ should be larger than the correlation length ξ. (In zigzag ribbons, the correlation length $\xi \sim \hbar v_F/\Delta$ is of the order of the lattice constant, estimated from the size of gap ~ 2 eV [8] and the Fermi velocity v_F). When the width increases, the size of ribbon and the ring must be increased at the same time. As a check on our method, we computed the TEE of a gapful armchair nanoribbon. We found the expected value of zero both in the absence and presence of disorder.

The TEE result of interacting disordered zigzag graphene nanoribbons is displayed in Fig. 4 for two values of the ring width. We see that, as the ring width increases, the numerical uncertainties decrease. We find that the numerical uncertainty of the computed TEE is small when the ring width is larger than $\gtrsim 7$ (it is estimated by varying the ring width at the fixed values of the ribbon length and width $L' \sim 300$ and $W \sim 100$ and the rectangular ring sizes $l_{\text{zig}} \sim 250$ and $l_{\text{arm}} \sim 50$).

Except for small values of Γ/U, the results are independent of different values of L', W, N_{imp}, l_{arm}, and l_{zig}. From the data collapse, we infer that $\beta \approx 0.016 \pm 0.003$ and that it is, within numerical uncertainty, *independent* of the strength of the interaction and disorder, i.e., independent of Γ/U. We consider this small value of β to be related to the presence of an exponentially small soft gap in interacting disordered ribbons [7]. We see from the data that, as the critical point is approached, $\Gamma/U \to 0$, the value of the TEE varies rather abruptly to zero in a nonuniversal manner [18]. (In limit of infinitely large systems, the transition should occur discontinuously at $\Gamma/U = 0$.)

In conclusion, our numerical work showed that the TEE of interacting disordered zigzag graphene nanoribbons is small but finite and universal. Disorder-free interacting zigzag graphene nanoribbons are in a critical phase that becomes

unstable in the presence of disorder. It would be interesting to find other systems with a pseudogap that belongs to the same universality class. It may be worthwhile to analytically compute S_{top} of a quasi-one-dimensional system in the presence of an exponentially small gap.

[1] K. S. Novoselov, A. K. Geim, S. V. Morozov, D. Jiang, M. I. Katsnelson, I. V. Grigorieva, S. V. Dubonos, and A. A. Firsov, Nature **438**, 197 (2005).

[2] Y. Zhang, Y. W. Tan, H. L. Stormer, and P. Kim, Nature **438**, 201 (2005).

[3] A. H. Castro Neto, F. Guinea, N. M. R. Peres, K. S. Novoselov, and A. K. Geim, Rev. Mod. Phys. **81**, 109 (2009).

[4] A. K. Geim and A. H. MacDonald, Phys. Today **60**(8), 35 (2007).

[5] P. Ruffieux, S. Wang, B. Yang, C. Sanchez-Sanchez, J. Liu, T. Dienel, L. Talirz, P. Shinde, C. A. Pignedoli, and D. Passerone, Nature **531**, 489 (2016).

[6] Y. H. Jeong, S.-R. Eric Yang, and M. C. Cha, J. Phys.: Condens. Matter **31**, 265601 (2019).

[7] S.-R. Eric Yang, M. C. Cha, H. J. Lee, and Y. H. Kim, Phys. Rev. Res. **2**, 033109 (2020).

[8] M. Fujita, K. Wakabayashi, K. Nakada, and K. Kusakabe, J. Phys. Soc. Jpn. **65**, 1920 (1996); L. Yang, C. H. Park, Y. W. Son, M. L. Cohen, and S. G. Louie, Phys. Rev. Lett. **99**, 186801 (2007).

[9] X.-G. Wen, Rev. Mod. Phys. **89**, 041004 (2017).

[10] X.-G. Wen, ISRN Condens. Matter Phys. **2013**, 198710 (2013).

[11] Y. H. Jeong, S. C. Kim, and S.-R. Eric Yang, Phys. Rev. B **91**, 205441 (2015).

[12] M. P. López-Sancho and L. Brey, 2D Mater. **5**, 015026 (2017).

[13] Y. H. Jeong and S.-R. Eric Yang, Ann. Phys. **385**, 688 (2017).

[14] L. Amico, R. Fazio, A. Osterloh, and V. Vedral, Rev. Mod. Phys. **80**, 517 (2008).

[15] S. M. Girvin and K. Yang, *Modern Condensed Matter Physics* (Cambridge University Press, Cambridge, 2019).

[16] J. Eisert, M. Cramer, and M. B. Plenio, Rev. Mod. Phys. **82**, 277 (2010).

[17] J. K. Pachos, *Introduction to Topological Quantum Computation* (Cambridge University Press, Cambridge, 2012).

[18] B. Zeng, X. Chen, D.-L. Zhou, and X.-G. Wen, *Quantum Information Meets Quantum Matter* (Springer, New York, 2019).

[19] A. Kitaev and J. Preskill, Phys. Rev. Lett. **96**, 110404 (2006).

[20] M. Levin and X.-G. Wen, Phys. Rev. Lett. **96**, 110405 (2006).

[21] H.-C. Jiang, Z. Wang, and L. Balents, Nat. Phys. **8**, 902 (2012).

[22] S.-R. Eric Yang and A. H. MacDonald, Phys. Rev. Lett. **70**, 4110 (1993).

[23] T. Stauber, P. Parida, M. Trushin, M. V. Ulybyshev, D. L. Boyda, and J. Schliemann, Phys. Rev. Lett. **118**, 266801 (2017).

[24] I. Peschel, J. Phys. A: Math. Gen. **36**, L205 (2003).

[25] J. I. Latorre and A. Riera, J. Phys. A: Math. Theor. **42**, 504002 (2009).